

# FLUKA applications in high energy problems: from LHC to ICARUS and atmospheric showers

A.Ferrari, T.Rancati and P.R.Sala

INFN sez. di Milano, and Milano University, via Celoria 16, I-20133 Milano, Italy

## Abstract

A few selected applications of FLUKA are illustrated. The ATLAS Combined calorimeter test beam is an example of calorimetric calculations, where all the physical models in the code are exploited in a fully analogue mode. The ATLAS radiation levels calculations are an impressive example of the use of biasing techniques together with the accuracy of neutron transport algorithms. The very high energy domain is well represented by state-of-the-art calculations of cosmic ray showers, whose ultimate goal is a detailed estimate of the atmospheric neutrino fluxes on earth. In neutrino physics, radionuclides are of serious concern, thus residual nuclei distributions due to muon photonuclear interactions in the Gran Sasso underground laboratory have been calculated.

## 1 Introduction

The field of application of FLUKA has exponentially grown from the original shielding calculation to a variety of running and future experiments. Our group is involved mainly in the ATLAS [2] and ICARUS [4] collaborations; both experiments are in the design and construction phase and therefore extensive simulations are needed for optimization and test beam analysis.

The simulation activity in the ATLAS framework is related to the calorimeter test beam data and to the radiation background studies. The analysis of the combined calorimeter test beam is presented as an example of the former item, while radiation levels for the most recent layout of the ATLAS detector and shielding configuration cover the latter item.

In ICARUS, FLUKA will be the official code for all optimization and data analysis tasks. Due to the specific needs of this future underground detector, many new physical processes and simulation tools have been and will be implemented in the code. Part of them are presented in another contribution to this conference. Here we report about a joint effort carried out by groups from the ICARUS and MACRO collaborations, which is of general interest, that is the calculation of atmospheric neutrino fluxes. This activity is still in a preliminary phase, but some interesting comparisons with experimental data on cosmic ray shower products in atmosphere are already available. A second ICARUS related application is again a background calculation, aimed to evaluate the amount and impact of radioactive nuclides produced by underground  $\mu$  interactions.

## 2 ATLAS combined calorimeter test beam

The future ATLAS experiment [2] at the CERN Large Hadron Collider (LHC) will include in the central ('barrel') region a calorimeter system composed of two separate units: a liquid argon (LAr) electromagnetic (EM) calorimeter, and a scintillating-tile hadronic calorimeter.

### 2.1 Experimental Setup

The first combined test of the two calorimeters was carried out at the CERN SPS in 1994 with the setup shown in fig. 1. The electromagnetic (EM) calorimeter was the Lead-Liquid Argon "2 metres" prototype built by the RD3 collaboration [5]. It has an accordion geometry, with a  $\Delta\phi \approx 0.02$ ,  $\Delta\eta \approx 0.018$  granularity, and it is fully pointing. The total thickness is  $25X_0$  at  $\eta = 0$ , subdivided into three longitudinal samplings. The resolution measured with electron beams is  $\frac{\sigma(E)}{E} = \frac{10\%}{\sqrt{E}} \oplus 0.5\%$  plus a noise term. In this test beam it was preceded by a  $3X_0$  thick separate preshower detector, also using LAr as active material [5, 6]. The need for a good coupling with the hadronic calorimeter compelled to shift the EM one toward the back of its cryostat, in a position that spoiled

its pointing properties. Behind the EM calorimeter the prototype of the Tile [7] hadronic (HAD) calorimeter was placed. This is an Iron-scintillator calorimeter, with an Fe:Sci ratio around five in volume. Its total thickness is 180 cm (about  $9 \lambda_i$ ) and it is read-out in 4 longitudinal sections. The Tile calorimeter was followed by a “muon wall”, consisting of an array of scintillator detectors. All data were taken on the H8 beam of the CERN SPS, with pion and electron beams of 20, 50, 100, 150, 200 and 300 GeV/c. A dedicated measurement with 300 GeV muons has also been performed [8]. The beam was impinging on the EM calorimeter at about  $11^\circ$ .

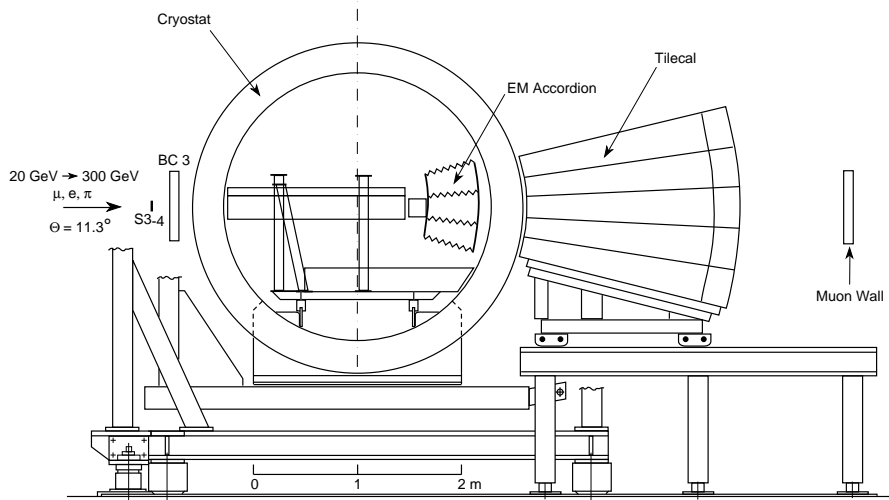


Figure 1: Test beam setup for the combined LAr and Tile calorimeter run.

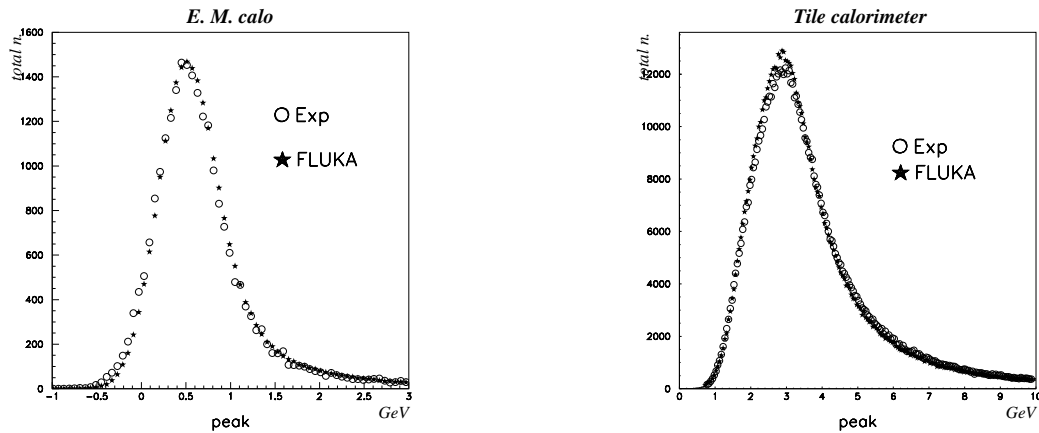


Figure 2: Absolute comparison between calculated and experimental ionization peaks in the electromagnetic(left) and hadronic (right) prototypes

## 2.2 Simulations

Simulations have been performed with FLUKA [1] and, independently, with GEANT3.21 [9], GCALOR [10] option. Here we describe FLUKA simulations, and present GEANT results for comparison. The setup and detector geometries have been modelled in great detail. The MonteCarlo calibration factors for the two detectors have been determined simulating the response to monoenergetic electrons. No other normalization factor has been applied to the simulated data. The effects of random noise and photostatistics have been convoluted with MC data, while charge collection in the accordion and quenching in the scintillator have been implemented directly in the simu-

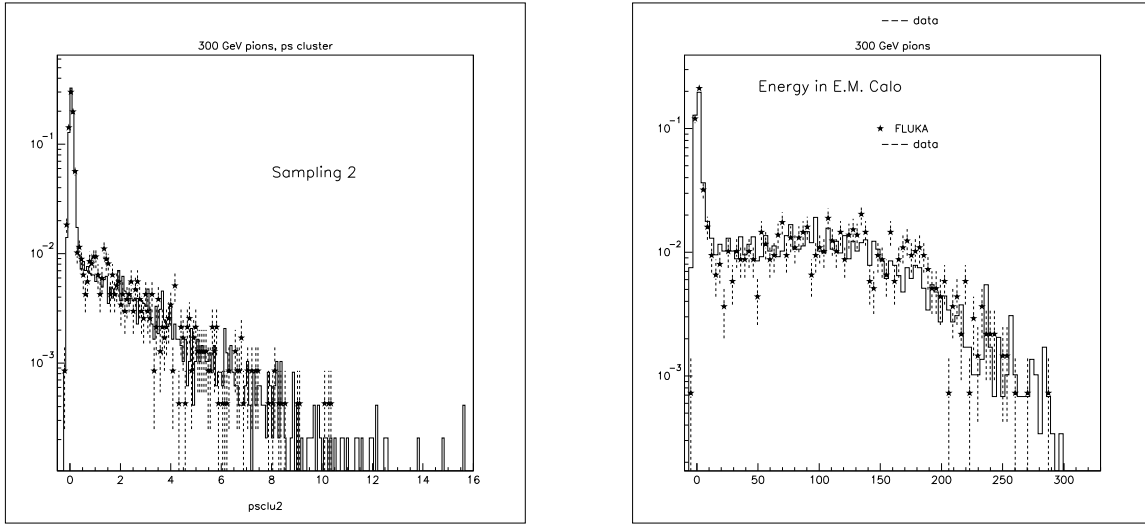


Figure 3: Absolute comparison between calculated and experimental energy depositions ( GeV ) in the second layer of the preshower (left) and in the EM calorimeter (right) for 300 GeV pions.

lations. An estimated 15% proton contamination has been added to the 20 GeV pion beam. As an example of the accuracy of the simulation, the ionization peaks for 300 GeV  $\mu$  are compared with data in fig. 2

### 2.3 Data analysis and results

The experimental data analysis employed both a simple method called “benchmark” and a more sophisticated “weighting” technique (see [3] for details ). The comparison with simulations has been done with the benchmark method. The total detected energy is reconstructed as the weighted sum of the accordion signal already calibrated in GeV in the electron scale  $E_{em}$  , the charge collected in the hadronic calorimeter  $Q_{had}$  , a correction factor to account for the energy lost in between the two calorimeters, and a negative correction term for highly electromagnetic showers:

$$E_0 = E_{em} + a \cdot Q_{had} + b \cdot \sqrt{|E_{em3} \cdot a \cdot Q_{had1}|} + c \cdot E_{em}^2 \quad (1)$$

the parameters  $a$ ,  $b$  and  $c$  were determined by minimizing the fractional energy resolution of 300 GeV pions. The last term was omitted when determining the  $e/\pi$  ratios. The signal from the preshower detector was used as a veto to discard events with early showers in dead materials. This first pass energy is then rescaled with a correction dictated by the noncompensating behaviour of the two calorimeters, following the approach of [11, 12]. The same procedure has been adopted for MC data analysis. It is interesting to note that the parameters resulting from the fit are very similar to the experimental ones: Assuming an experimental electron scale calibration factor of 5.59 pC/GeV [13] and using the same notation of eq. 1 the parameters are:  $a=0.96/5.59=0.172\pm 0.002$  GeV/pC,  $b=0.38\pm 0.02$  and  $c=-0.00038\pm 0.0001$  GeV $^{-1}$ , while the experimental ones were:  $a = 0.172$  GeV/pC,  $b = 0.44$  and  $c = - 0.00038$  GeV $^{-1}$ .

Comparisons between experimental and simulated data for shower developments are presented in figs. 3 and 4, while for  $e/\pi$  ratios and fractional resolution in fig. 5 and fig. 6 respectively. These comparisons were both a benchmark of the calculations and an important help in order to understand a few experimental problems. Indeed, the excellent agreement of FLUKA calculation with experimental shower developments washed out the doubt on data quality that arose from the earlier GEANT results. Moreover, the observed broadening of the resolution at low energies, with an anomalous increase of the fitted noise term well above the 1.6 GeV rms extracted from random trigger events, could be attributed partially to proton contamination (increases the resolution by a factor  $\approx 1.07$  at 20 GeV from FLUKA), and partially to the effect of dead materials coupled to a non perfect preshower veto.

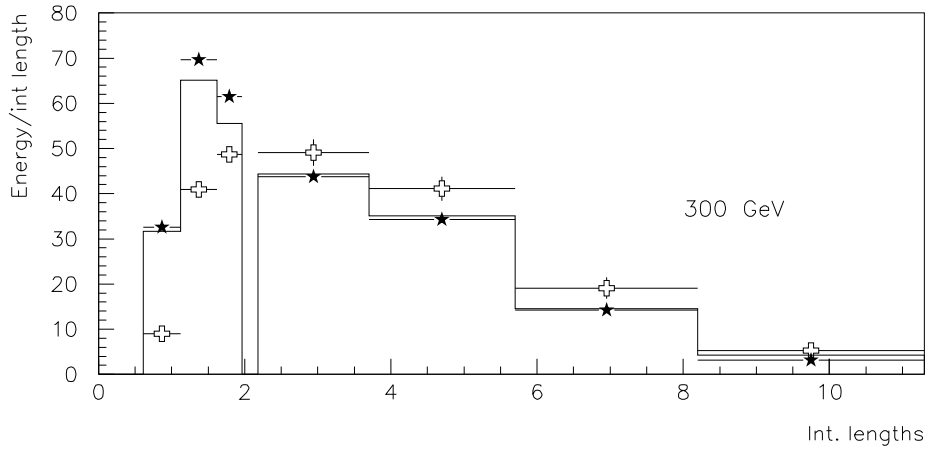
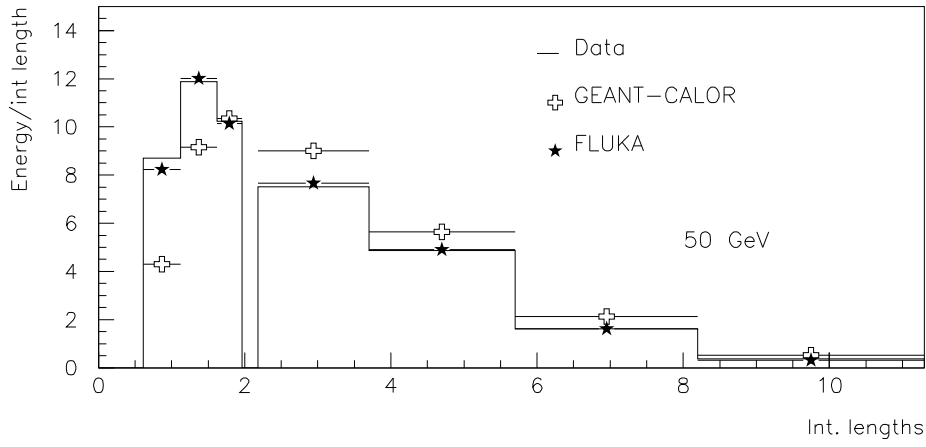


Figure 4: Longitudinal shower developments for 50 and 300 GeV pions

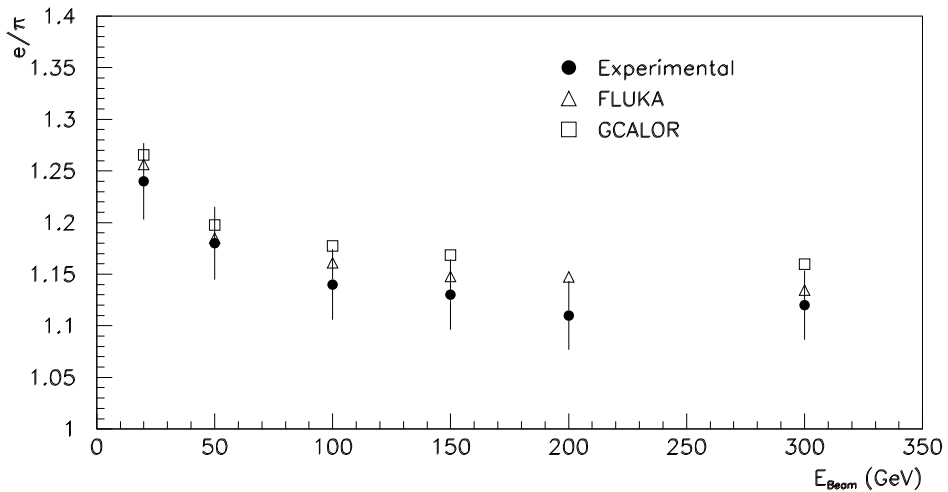


Figure 5:  $e/\pi$  ratio

### 3 ATLAS background

ATLAS is one of the detectors to be installed at the future proton-proton collider LHC. Due the high luminosity ( $1 \cdot 10^{34} \text{cm}^{-2} \text{sec}^{-1}$ ) and center of mass energy (7+7 TeV) foreseen at LHC, the level of background is one of the major problems for the detectors.

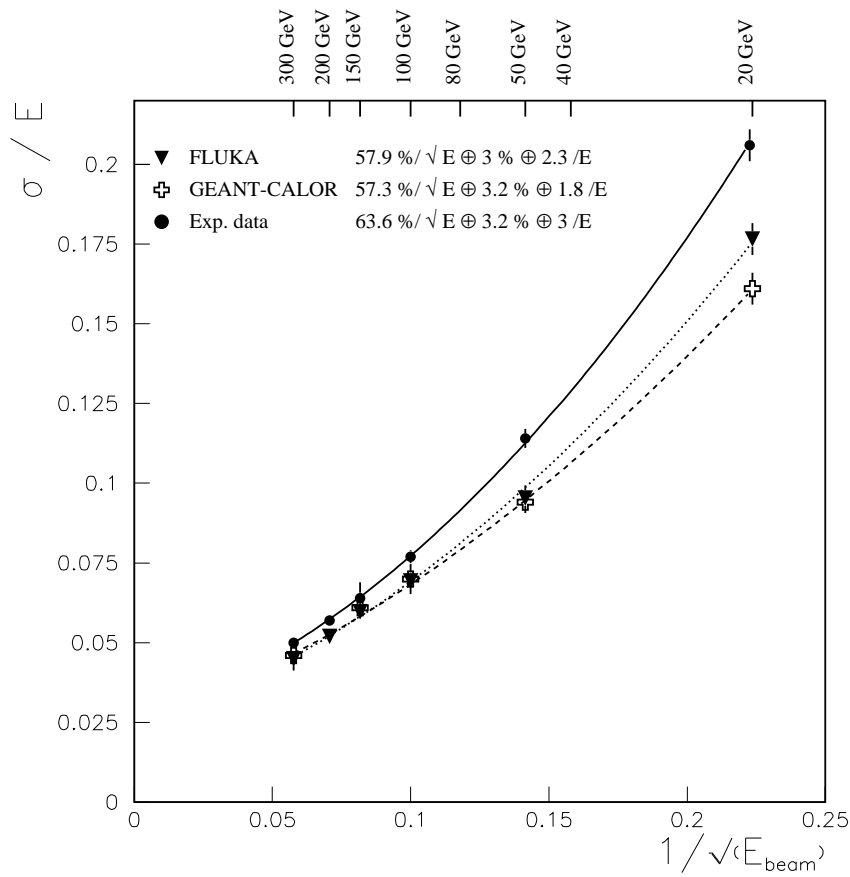


Figure 6: Fractional resolutions

Table 1: Altitude variation of multi-sphere neutron spectrometer rates: comparison between experimental and FLUKA results.

Poly radius (cm)	Altitude					
	0 m		4880 m		11280 m	
	EXP ( $s^{-1} \pm err\%$ )	FLUKA ( $s^{-1} \pm err\%$ )	EXP ( $s^{-1} \pm err\%$ )	FLUKA ( $s^{-1} \pm err\%$ )	EXP ( $s^{-1} \pm err\%$ )	FLUKA ( $s^{-1} \pm err\%$ )
0	$2.40 \cdot 10^{-2} \pm 12$	$4.15 \cdot 10^{-2} \pm 5$	$0.43 \pm 9$	$0.181 \pm 1$	$2.61 \pm 6$	$0.976 \pm 1$
4.1	$2.30 \cdot 10^{-2} \pm 12$	$2.74 \cdot 10^{-2} \pm 4$	$0.570 \pm 4$	$0.585 \pm 1$	$3.31 \pm 4$	$3.09 \pm 1$
5.6	$2.90 \cdot 10^{-2} \pm 11$	$3.27 \cdot 10^{-2} \pm 3$	$0.753 \pm 7$	$0.949 \pm 1$	$4.5 \pm 4$	$4.99 \pm 1$
7.6	$3.53 \cdot 10^{-2} \pm 10$	$3.51 \cdot 10^{-2} \pm 3$	$0.860 \pm 6$	$1.06 \pm 1$	$5.01 \pm 3$	$5.55 \pm 1$
11.6	$2.03 \cdot 10^{-2} \pm 13$	$2.71 \cdot 10^{-2} \pm 3$	$0.620 \pm 7$	$0.708 \pm 1$	$3.35 \pm 4$	$3.67 \pm 1$
22.6	$8.14 \cdot 10^{-3} \pm 13$	$1.20 \cdot 10^{-2} \pm 3$	$0.177 \pm 10$	$0.215 \pm 1$	$1.09 \pm 7$	$1.13 \pm 1$

Simulations have been extensively performed to evaluate the radiation levels, to optimize the shielding, and to estimate the effect on the various subdetectors in terms of damage and occupancy [15].

The large attenuation factors due to the detector itself and to the shielding call for an extensive use of several biasing techniques in order to keep the CPU time within reasonable limits. These techniques must be coupled to a very accurate shower simulation, from minimum bias production down to thermal neutron and capture  $\gamma$  rays. Examples of the results with the last detector/shielding configuration are shown in fig. 7 for the damage to the silicon tracker, and fig. 8 for the photon background in the muon system.

## 4 Cosmic rays

Recent results on atmospheric neutrino experiments [16] show a significant disagreement with theoretical expectations on the ratio of muon-to-electron (anti)-neutrinos produced by cosmic rays interacting in the earth atmosphere. The absolute value of  $\nu$  fluxes is of key importance in strengthening or not the interpretation in terms

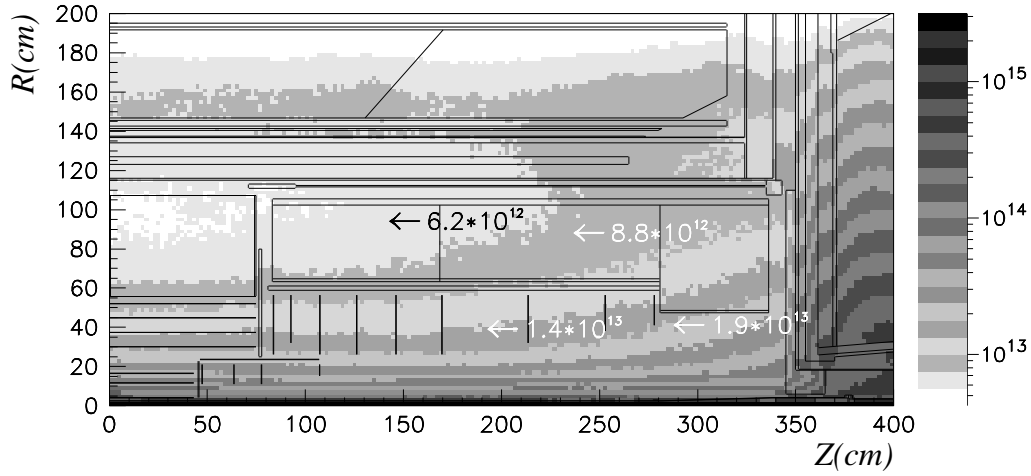


Figure 7: Total silicon damage (1 MeV equivalent neutrons  $\text{cm}^{-2} \text{y}^{-1}$ ) expected in the ATLAS inner detector

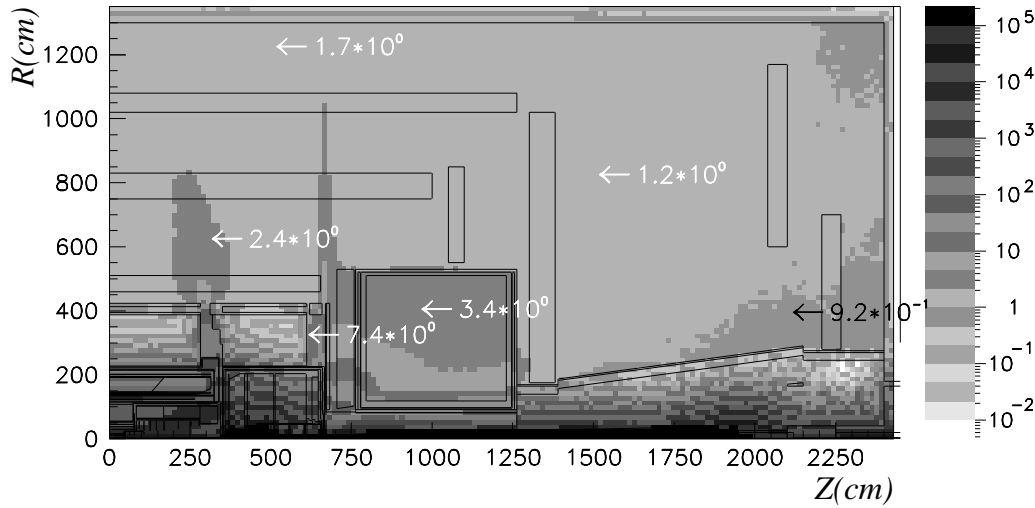


Figure 8: Instantaneous photon fluence ( $\text{kHz cm}^{-2}$ ) expected in the ATLAS hall

of  $\nu$  oscillations, and in giving hints about which  $\nu$  flavors are involved in the oscillation mechanism. Despite several calculations of  $\nu$  fluxes exists, there is still room for tests and improvements. A simulation plan has been initialized, with two possible major improvements with respect to previous ones: the use of a fully tridimensional geometry instead of the usual monodimensional approximation, and the exploitation of the FLUKA hadronic interaction models.

The input primary cosmic ray spectra are interstellar proton and ion spectra [17], modulated by the solar wind. Ions (up to Nickel) are splitted in nucleons at the top of the atmosphere. The vertical geomagnetic cutoffs are taken from a worldwide tabulation [14], and converted to different incident angles using the Störmer approximation. The use of a detailed description of the earth magnetic field in terms of a numerical multipole expansion is foreseen in

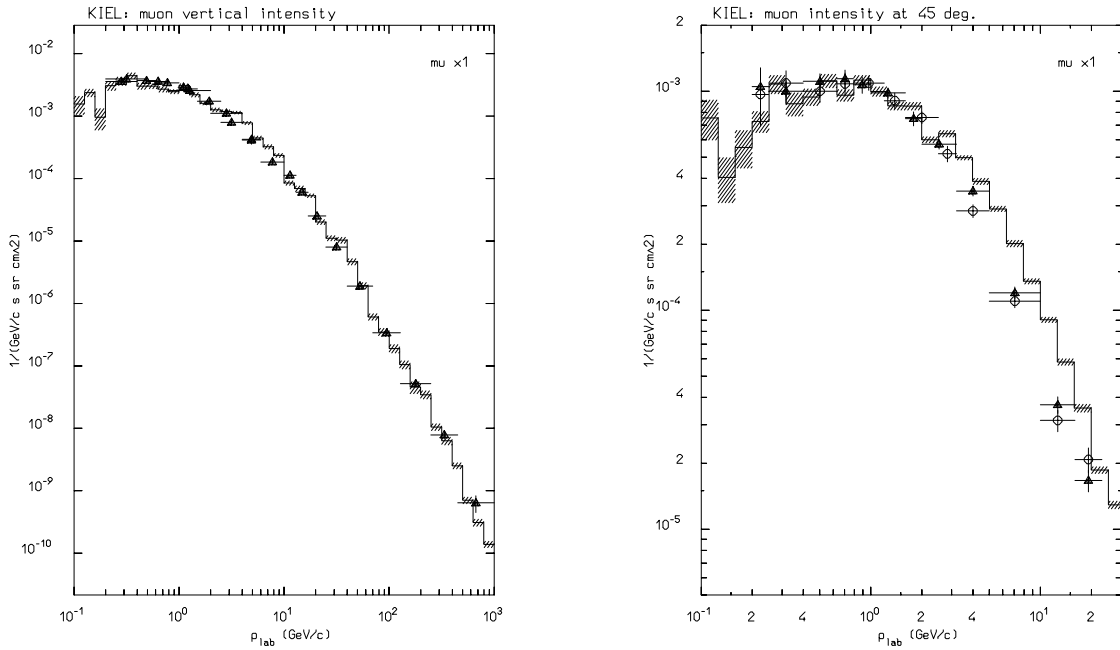


Figure 9: Muon spectra at sea level, at vertical incidence (left) and at  $45^\circ$  incidence. Dashed histogram : FLUKA results with errors, symbols : data. In the rightmost plot, the closed triangles are muons from east, open dots  $\mu$  from west [18, 19]

a later stage.

We present here preliminary comparisons with experimental data on various shower components in atmosphere, at different geomagnetic latitudes, altitudes and angles of incidence.

Muon spectra have been measured by several groups in different geographical locations. The experiment of Allkofer and collaborators [18, 19] is one of the few that took data also at a non vertical angle of incidence, thus it is a more stringent test of the production mechanisms, angular distributions and geometrical models. The measurements have been performed in Kiel ( $54^\circ\text{N } 10^\circ\text{E}$ ) in the years around 1967 at sea level, with three magnetic spectrometers covering together the range 0.2- 1000 GeV/c, at vertical and  $45^\circ$  incidence. The results of the simulation are presented in fig. 9.

As an example of neutron production at different altitudes, the experiment of Nakamura and coworkers [20] has been simulated. The measurements have been performed on an aircraft at and above the Narita airport (latitude in the range  $33.44^\circ\text{N}$  and  $35.77^\circ\text{N}$ , longitude  $133.68^\circ\text{E}$ - $140.96^\circ\text{E}$ ) the 27<sup>th</sup> February 1985. Neutrons were detected with a Bonner spectrometer made up by 5 polyethylene spheres (from 81 to 451 mm in radius) each surrounding a  $^3\text{He}$  detector, and with a bare  $^3\text{He}$  tube. The results of simulations have been obtained by a convolution of the calculated neutron spectra with the calculated response functions of the spheres. The comparison with experimental data at sea level, at 4880 m and at 11280 m, is presented in table 1. The agreement is good except for the bare detector, whose response is likely to be biased by the aircraft walls and interiors, that were not reproduced in the simulations.

## 5 Cosmic Muons and radionuclides under Gran Sasso

Muons produced by cosmic rays still survive after traversing the rock that shields the Gran Sasso laboratory. The measured muon rate is about  $1\mu/m^2h$  with an average energy of about 280 GeV. These muons can produce radioactive nuclides directly inside the detectors via photonuclear interactions. Isotopes with a decay time larger than typical veto time windows, and a detectable decay energy represent a dangerous background source, especially for low energy events such as the solar neutrino ones. A calculation has been performed with FLUKA for a 600 Ton LAr ICARUS module in the Gran Sasso hall C, using as input a typical underground muon spectrum [21].

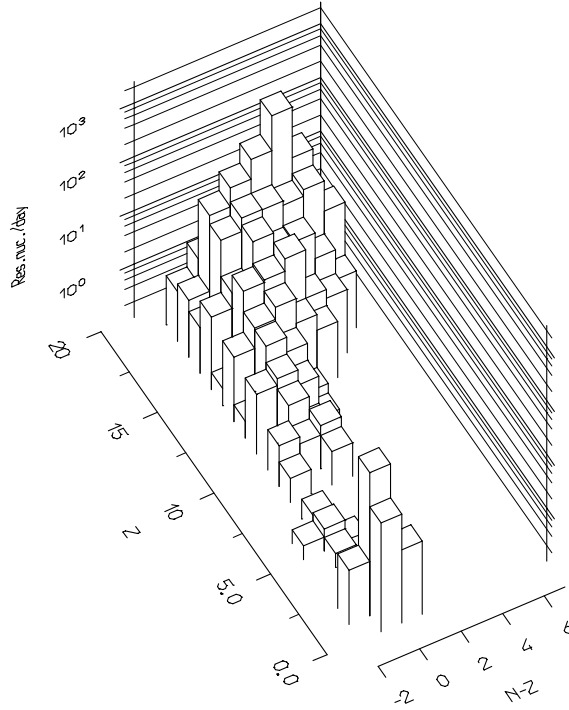


Figure 10: Expected residual nuclei (number/day) from muon photonuclear interactions in the ICARUS 600 Ton detector as a function of atomic number  $Z$  and neutron excess  $N-Z$

Table 2: Most dangerous residual nuclei produced per day by  $\mu$  photonuclear interactions in a 600 Ton LAr tank

Isotope	number/day	$T_{1/2}$	Decay type	Q-value ( MeV)
$^{40}\text{Cl}$	$11 \pm 13\%$	1.4 m	$\beta^-$	7.5
$^{38}\text{Cl}$	$30 \pm 14\%$	37.3 m	$\beta^-$	4.91
$^{34}\text{Cl}$	$0.7 \pm 50\%$	1.56 s	$\beta^+$	5.48
$^{34m}\text{Cl}$		32 m	$\beta^+, \text{IT}$	

The map of residual nuclei is shown in fig. 10. An estimate of potentially dangerous nuclides and their properties is collected in table 2. Only isotopes with decay Q-values comparable with the planned ICARUS detection threshold for solar neutrino events, around 5 MeV kinetic energy, have been taken into account. The impact on solar neutrino detection has to be investigated.

## References

- [1] A. Fassò, A. Ferrari, J. Ranft and P.R. Sala, Proc. of the workshop on *Simulating Accelerator Radiation Environment*, SARE, Santa Fè, 11-15 january (1993), A. Palounek ed., Los Alamos LA-12835-C (1994) 134;  
 A. Fassò, A. Ferrari, J. Ranft and P.R. Sala, Proc. of the *IV International Conference on Calorimetry in High Energy Physics*, La Biodola (Elba), September 19-25 1993, A. Menzione and A. Scribano eds., World Scientific (1994) 493;  
 A. Fassò, A. Ferrari, J. Ranft and P.R. Sala, Proc. of the *Specialists' Meeting on Shielding Aspects of Accelerators, Targets & Irradiation Facilities*, Arlington, April 28-29 1994, published by OECD/NEA (1995) 287;  
 A. Fassò, A. Ferrari, J. Ranft and P.R. Sala, Proc. of the 2nd workshop on *Simulating Accelerator Radiation*

- Environment*, SARE-2, CERN-Geneva, October 9–11 1995,;  
A. Ferrari and P.R. Sala, *The Physics of High Energy Reactions*, Proc. of the *Workshop on Nuclear Reaction Data and Nuclear Reactors Physics, Design and Safety*, International Centre for Theoretical Physics, Miramare-Trieste, Italy, 15 April–17 May 1996, World Scientific in press.
- [2] Technical Proposal of the ATLAS collaboration, CERN/LHCC/94-43,
- [3] Z. Ajaltouni et al. (ATLAS collaboration), CERN-PPE/96-178 and accepted for publication in *Nucl. Instr. Meth. A*.
- [4] P. Cennini et al. ( ICARUS coll.) ICARUS II, Experiment proposal Vol. I & II, LNGS-94/99-I&II
- [5] D.M. Gingrich et al. ( RD3 collaboration), *Nucl. Instr. Meth.* **A364**, 290 (1995).
- [6] R.A. Davis et al. (RD3 collaboration), *Nucl. Instr. Meth* **A385** , 47 ( 1997)
- [7] F. Ariztizabal et al, *Nucl. Instr. Meth* **A349**, 384 (1994)
- [8] M. Antonelli et al., proceedings of the *VI International conference in High Energy Physics*, Frascati Physics Series pag. 561 (1997)
- [9] R. Brun and F. Carminati, *GEANT Detector Description and Simulation Tool*, CERN Program Library, Long Writeup W5013, September 1993.
- [10] C. Zeitnitz and T.A. Gabriel, *The GEANT–CALOR Interface User’s Guide*, GCALOR version 1.04/07.
- [11] D.E. Groom, Proc. of the *II International Conference on Calorimetry in High Energy Physics*, Capri 1991, (ed. A. Ereditato) World Scientific pag. 376 (1992).
- [12] T.A. Gabriel, D.E. Groom, P.K. Job, N.V. Mokhov and G.R. Stevenson, *Nucl. Instr. and Meth.* **A338** (1994) 336.
- [13] J.A. Budagov et al., ATLAS Internal Note TILECAL-NO-72 (1995)
- [14] M. A. Shea and D. F. Smart, report no. AFCRL-TR-75-0185, HANSCOM AFB, MASS., 1975.
- [15] G. Battistoni, A. Ferrari, and P.R. Sala, *Background calculations for the ATLAS detector and hall* Atlas internal note ATLAS-GEN-010, October 1994, and addendum, January 1995.; A. Ferrari, G. Battistoni and P.R. Sala, *Muon Chamber Sensitivity to neutron and photon background in the ATLAS hall*, Atlas internal note ATLAS-MUON-NO-052 (1994); A. Ferrari, K. Potter and S. Rollet, *Shielding for the ATLAS Experimental Region*, LHC Project Note 6 (1995).
- [16] K.S. Hirata et al., *Phys. Lett.* **B 205** 416 ( 1988); **B 280** 146 ( 1992); Y. Fukuda et al.,*Phys. Lett.* **B 335** 237 ( 1994); P.J. Litchfield, Proc. Int. Europhys. Conf on High Energy Physics ( Marseille 1993), ed J. Carr and M. Perrotet, Edition Frontieres, Gif-sur-Yvette, pag.557; R. Becker-Szendy et al., *Phys. rev.* **D 46** 3720 (1992); D. Casper et al., *Phys. Rev. Lett* **66** 2561 (1992)
- [17] P.M. O’Neill, Program HIZ, private communication of L. Pinsky, Houston University.
- [18] O.C. Allkofer, K. Cartesen and W.D. Dau, *Phys. Lett.* 36B(4), 425 (1971)
- [19] O.C. Allkofer and R.D. Andresen, *Il Nuovo Cimento LI B*(2), 329 (1967)
- [20] T. Nakamura et al., *Health Phys.* **53** 509 (1987)
- [21] T.K. Gaisser, “ Cosmic Rays and Particle Physics”, Cambridge University Press (1990).